



Identification and optimisation of 4,5-dihydrobenzo [1,2-*d*:3,4-*d*]bisthiazole and 4,5-dihydrothiazolo[4,5-*h*]quinazoline series of selective phosphatidylinositol-3 kinase alpha inhibitors

Robin A. Fairhurst*, Marc Gerspacher, Patricia Imbach-Weese, Robert Mah, Giorgio Caravatti, Pascal Furet, Christine Fritsch, Christian Schnell, Joachim Blanz, Francesca Blasco, Sandrine Desrayaud, Daniel A. Guthy, Mark Knapp, Dorothee Arz, Jasmin Wirth, Esther Roehn-Carnemolla, Van Huy Luu

Novartis Institutes for BioMedical Research, Global Discovery Chemistry, Novartis Pharma AG, Werk Klybeck, Postfach, CH-4002 Basel, Switzerland

ARTICLE INFO

Article history:

Available online 26 June 2015

Keywords:

Oncology
Kinase inhibitor

Phosphatidylinositol-3-kinase-alpha

ABSTRACT

A cyclisation within a 4',5'-bisthiazole (*S*)-proline-amide-urea series of selective PI3K α inhibitors led to a novel 4,5-dihydrobenzo[1,2-*d*:3,4-*d*]bisthiazole tricyclic sub-series. The synthesis and optimisation of this 4,5-dihydrobenzo[1,2-*d*:3,4-*d*]bisthiazole sub-series and the expansion to a related tricyclic 4,5-dihydrothiazolo[4,5-*h*]quinazoline sub-series are described. From this work analogues including **11**, **12**, **19** and **23** were identified as potent and selective PI3K α inhibitor in vivo tool compounds.

© 2015 Elsevier Ltd. All rights reserved.

Phosphatidylinositol-3-kinase alpha (PI3K α) is a member of the class 1 PI3K family which has been strongly implicated as a key driver in a number of cancers through amplification, overexpression and mutation.¹ In particular, PI3K α is one of the most commonly mutated genes in human cancer, and these mutations typically lead to enhanced, or constitutive, PI3K α kinase-activity.² As a result several groups have sought to identify selective PI3K α inhibitors to explore as anticancer treatments. Of these the (*S*)-proline-amide aminothiazole-urea derivative alpelisib is currently one of the most advanced with Phase I/II clinical studies currently ongoing.³

In the preceding Letter we described the identification of a 4',5'-bisthiazole variant of an (*S*)-proline-amide aminothiazole-urea series, as exemplified by A66 in Figure 1.⁴ This formed part of a broader piece of work which started from the hit structures, exemplified by **1** in Figure 2, and culminated in the identification of alpelisib.^{5,6} In this Letter we describe an additional extension of this work in which a further annulation was introduced to generate the tricyclic 4,5-dihydrobenzo[1,2-*d*:3,4-*d*]bisthiazole core, as exemplified by the general structure **2**.

Expanding upon the homology modeling that was carried out with the 4',5'-bisthiazole analogues, such as A66, suggested an opportunity to increase the interaction within the ATP pocket of PI3K α .⁴ A cyclization from the 4-methyl of the aminothiazole

moiety to close a 6-membered ring onto the unsubstituted position of the second thiazole ring yielded the general structure **2**. This cyclisation was anticipated to introduce additional favorable hydrophobic contacts within the affinity pocket with the side-chain of tyrosine 836, as shown in Figure 3. Additionally, the cyclisation also locks the inhibitor in the conformation required for optimally interacting within the PI3K ATP-pocket. However, the low energy conformation of the 4',5'-bisthiazole biaryl-bond corresponds closely to the locked conformation, and a negligible contribution was anticipated from limiting the conformational mobility about the bisthiazole linkage. At the initiation of this work, a similar cyclisation had also been reported for a related series of aminothiazole tricyclic PI3K inhibitors.⁷

To prepare the analogues **2**, a synthesis was developed starting from 2-bromo-1,3-cyclohexanedione.⁸ Annulation with thiourea introduced the 2-aminothiazole moiety which was *N*-acylated to give **3**. Bromination of the remaining ketone functionality was followed by formation of the second thiazole ring upon heating with a range of thioamides, to give the analogues **4**, in a reaction catalysed by ammonium phosphomolybdate.⁹ Hydrolysis of the acetamide moiety was followed by preparation of the acylimidazole intermediates, which were isolated and then reacted with the appropriate proline-amide derivatives to give the targeted compounds **5–12**, of the general structure **2**.

Table 1 shows the biochemical and cellular data for A66 and the cyclised analogues **5–12**.¹⁰ Comparison of A66 with the corresponding cyclised analogue **5** shows the impact of the cyclisation on class 1 PI3K activity: similar levels of biochemical activity and

* Corresponding author. Tel.: +41 61 69 64294; fax: +41 61 6966246.

E-mail address: robin.fairhurst@novartis.com (R.A. Fairhurst).

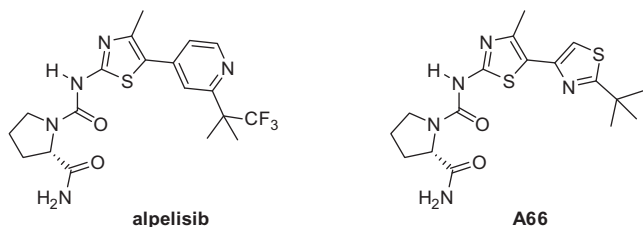


Figure 1. Structures of the PI3K α (S)-proline-amide aminothiazole-urea derivatives alpelisib and A66.

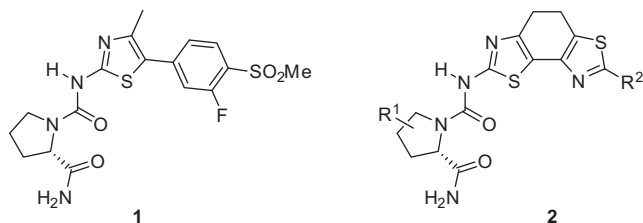


Figure 2. Structures of the proline-amide-urea series starting point **1** and the proposed cyclised 4,5-dihydrobenzo[1,2-*d*:3,4-*d*]bisthiazole analogues **2**.

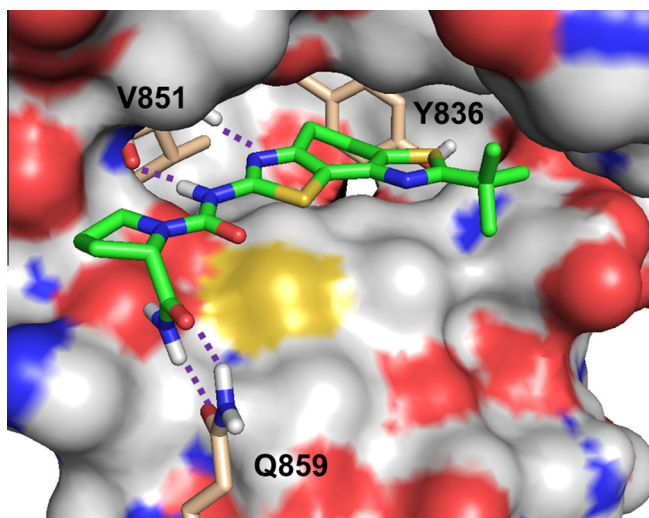


Figure 3. Model of a cyclised version of A66 corresponding to the proposed series **2**, compound **5**, docked in the ATP binding site of PI3K α based on the crystal structure of the enzyme in complex with alpelisib (PDB code: 4JPS). Key hydrogen bonds are represented as dashed lines.

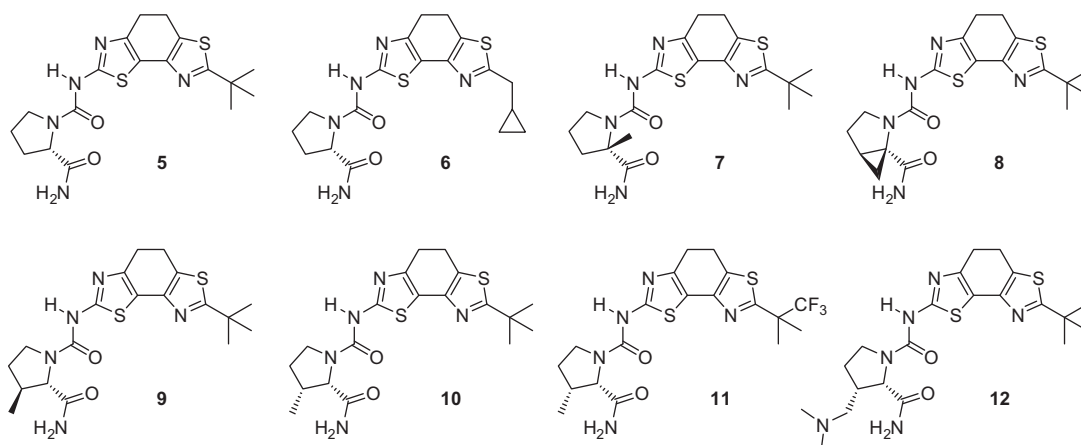
selectivity were determined for both compounds, but a greater level of cellular PI3K α activity was measured for the cyclised analogue **5**. This observation, of increased PI3K activity for the cyclised analogues, particularly at the cellular level, is seen throughout the series and supports the hypothesised favorable interaction of the additional ring-methylene with the conserved Y836 residue (PI3K α numbering). The increased cellular activity was especially interesting because during the optimisation of the series it was found to be the best predictor of *in vivo* potency and selectivity. Evaluating the level of plasma protein binding (PPB) for the cyclised series showed similar levels to the acyclic analogues when predicted from the human and rat serum albumin binding (HSA and RSA), Table 2.¹¹ Thus, indicating the increase in cellular activity, relative to the biochemical activity, between the two series not to be driven by a change in unbound fraction.⁴ The structure

activity relationships (SAR) for the affinity-pocket 2-thiazole ring was found to be comparable to that observed for the parent series. Small quaternary alkyl residues led to the highest levels of activity, as exemplified by comparing the isomers **5** and **6**, consistent with optimally filling the affinity pocket.⁴ Similarly, the substituted proline SAR was mirrored in the cyclised analogues, as exemplified by compounds **7–11**. In particular, the *trans*- and *cis*-3-methyl proline analogues led to some of the most highly potent and selective examples prepared in the entire series, with cellular PI3K α activities below 10 nM and selectivities of greater than 50-fold versus the other class 1 PI3K's. Building on this observation, the potential for incorporating a tertiary amine into the proline nucleus, as a solubility enhancing functionality, was explored. One successful example was the *cis*-3-dimethylaminomethyl proline analogue **12**, the key building block for which was prepared via an extension of a reported amino-zinc-enolate-cyclisation.^{12,8} Compound **12** resulted in a potent and selective PI3K α inhibitor substituted with a tertiary amine, something which had proven to be difficult to achieve in the parent 4',5-bisthiazole sub-series.⁴

Evaluating the physical properties of the 4,5-dihydrobenzo[1,2-*d*:3,4-*d*]bisthiazole analogues **2**, the increase in PI3K α potency led to a favorable impact upon the perceived pharmacokinetic (PK) risk by reducing the anticipated level of exposure required to achieve efficacy. This was helpful as the low solubility of the 4',5-bisthiazole series, which had been attributed as one of the primary reasons for the low oral bioavailabilities, was not significantly improved upon by the cyclisation, when direct analogues were compared between the series.⁴ Solubilities determined at pH 6.8 for the most potent 3-methyl analogues **9–11** were all below 14 μ M.¹³ However, for the direct A66 analogue, compound **5**, a slightly higher solubility of 65 μ M was determined, in combination with high permeability and also a good level of metabolic stability.^{14,15} A rat PK study with **5** resulted in an encouraging exposure profile, and a respectable oral bioavailability of 38%, when administered as a suspension at a dose of 3.0 mg kg⁻¹. The PK data for selected compounds are summarised in Table 3.¹⁶ The more soluble basic analogue **12** also showed a good level of metabolic stability with a moderate level of permeability that was associated with a modest efflux signal in a Caco-2 monolayer assay.¹⁴ Exploring further, a rat PK study with **12** also resulted in an encouraging level of oral bioavailability of 56%, and a long half-life, driven by the higher volume of distribution. However, in contrast to the other analogues in Table 1, compound **12** showed significant inhibition of dofetilide binding to the human ether- α -go-go related gene ion-channel (hERG), with an IC₅₀ of 5.7 μ M, which deprioritised further follow up for this compound. Overall, these data suggested improved PK profiles were possible for the cyclised analogues **2**, at least at low dose levels below that expected to deliver efficacy, which encouraged further follow up studies for the most interesting examples, such as compound **11**.

On the basis of the favorable outcome of the cyclisation leading to the 4,5-dihydrobenzo[1,2-*d*:3,4-*d*]bisthiazole series **2**, the same strategy was also applied to the proline-amide-urea sub-series containing a pyrimidyl affinity-pocket binder, as exemplified by compound **13**.^{3,5} Applying the same annulation leads to the 4,5-dihydrothiazolo[4,5-*h*]quinazoline analogues of the general structure **14**, as depicted in Figure 4.

The analogues **14** were readily prepared, and starting from the *N*-acylated 2-aminothiazole-fused cyclohexanone **3** was found to be the most efficient route, as outlined in Scheme 2.⁸ Formylation of the lithium enolate of **3** with methyl formate gave the β -ketoaldehyde **15** in high yield. Subsequent reaction of **15** with a range of amidines generated the pyrimidine containing tricyclic core, which was followed by acetamide hydrolysis to give the key intermediates **16**. Conversion of these 2-aminothiazole intermediates **16** into the final proline-amide-urea targets was

Table 1
PI3K α , PI3K β , PI3K γ and PI3K δ activities for A66 and the 4,5-dihydrobenzo[1,2-d:3,4-d]bisthiazole analogues 5–12

Compound	Biochemical IC ₅₀ (μM)				Cellular IC ₅₀ (μM)		
	PI3K α	PI3K β	PI3K γ	PI3K δ	PI3K α	PI3K β	PI3K δ
A66	0.015	6.5	8.0	1.5	0.20	>10	>10
5	0.013	2.5	0.16	0.70	0.019	3.6	1.4
6	0.070	5.1	1.1	1.6	0.19	1.3	3.4
7	0.008	0.72	n.d.	n.d.	0.028	1.2	4.0
8	0.009	4.5	8.0	5.6	0.011	>10	>10
9	0.013	1.8	0.33	0.91	0.010	0.45	1.0
10	0.011	2.3	0.20	1.0	0.010	1.0	1.5
11	0.009	0.93	0.16	0.23	0.005	0.98	0.59
12	0.010	5.5	0.99	0.97	0.025	>10	4.0

n.d. not determined.

Table 2
Physicochemical and in vitro PK data for selected reference compounds and proline-amide-urea aminothiazole derivatives

Compound	clogP/PSA (Å ²)	Sol. pH 6.8 (μM)	HDM FA (%)	Caco-2 A-B/B-A (10 ⁻⁶ cm s ⁻¹)	Rat microsome Cl (μl min ⁻¹ mg ⁻¹)	HSA/RSA (%)
Alpelisib	2.1/101	53	89	3.8/18.3	29	90.0/92.7
A66	2.5/101	90	96	12.3/15.6	126	n.d.
5	2.8/101	65	93	n.d.	37	91.9/92.6
6	2.4/101	55	57	n.d.	26	95.3/95.0
7	3.3//101	310	93	12.1/15.6	73	91.9/92.1
8	2.5/101	351	76	n.d.	96	n.d.
9	3.3/101	< 4	91	n.d.	100	n.d.
10	3.3/101	9	95	n.d.	80	n.d.
11	2.9/101	14	86	n.d.	34	n.d.
12	2.1/104	n.d.	30	0.76/6.87	18	n.d.
17	2.0/114	125	63	n.d.	34	n.d.
18	2.5/114	60	84	3.4/25.5	33	90.3/n.d.
19	1.8/114	51	50	n.d.	31	87.8/94.9
20	2.5/114	71	45	3.4/21.7	n.d.	90.4/94.2
21	2.2/14	9	52	n.d.	18	n.d.
22	1.3/117	276	n.d.	n.d.	3	n.d.
23	2.5/117	>1000	80	5.2/15.8	58	78.7/87.9
24	1.9/117	500	29	n.d.	53	89.7/94.5

clogP was calculated using clogP version 7.4, BioByte Corporation.

Table 3
Pharmacokinetic data for selected proline-amide-urea aminothiazole derivatives

Compound	CL (mL min ⁻¹ kg ⁻¹)	V _{ss} (L kg ⁻¹)	Terminal half-life (h)	iv AUC d.n. (nmol h L ⁻¹)	p.o. AUC d.n. (nmol h L ⁻¹)	Bioavailability (%)
A66	74 ± 14	2.0 ± 0.4	0.3 ± 0.1	561 ± 101	70 ± 16	2.0 ± 1.0
5	10 ± 1	0.4 ± 0.0	1.5 ± 0.2	4132 ± 304	1585 ± 388	39 ± 9
12	39 ± 11	24 ± 11	9.6 ± 2.8	956 ± 227	531	56
13	42 ± 14	1.3 ± 0.3	1.9 ± 0.9	1128 ± 376	199 ± 111	18 ± 10
19	3 ± 0	0.6 ± 0.1	3.7 ± 0.3	16472 ± 3211	13599 ± 4065	83 ± 25
20	8 ± 1	0.5 ± 0.2	1.1 ± 0.2	5241 ± 589	1874 ± 917	36 ± 17
23	26 ± 3	3.2 ± 0.1	2.0 ± 0.1	1444 ± 190	1116 ± 234	77 ± 16

d.n. = dose normalised to 1.0 mg kg⁻¹.

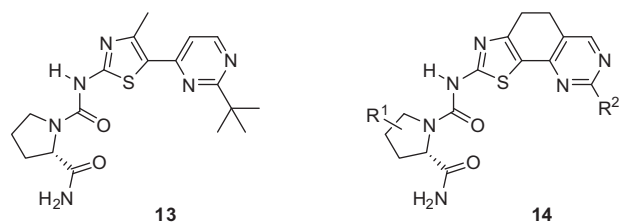
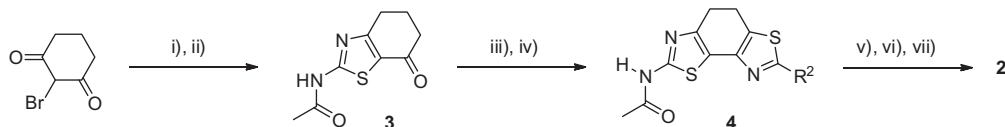


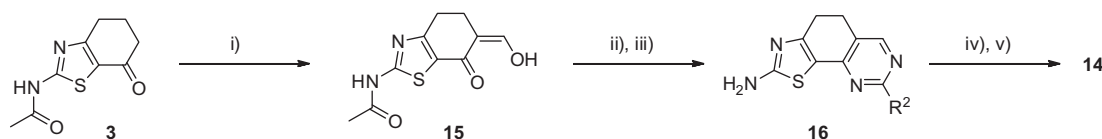
Figure 4. Expansion to a 4,5-dihydrothiazolo[4,5-*h*]quinazoline series **14**: comparison with the acyclic pyrimidine series, as exemplified by compound **13**.

achieved following the same two-step protocol outlined in [Scheme 1](#).

[Table 4](#) shows the biochemical and cellular data for compound **13** and the cyclised analogues **17–24**, corresponding to the general structure **14**.¹⁰ Consistent with the observations made for series **2**, the SAR was also found to track well from the biaryl analogues to the tricyclic series **14**, and as anticipated a significant increase in potency, in particular cellular potency, was associated with the cyclised series. For example, the direct cyclised analogue of **13**, compound **17**, showed a 7-fold increase in cellular PI3K α potency. However, some erosion of the PI3K α selectivity (<5-fold) was



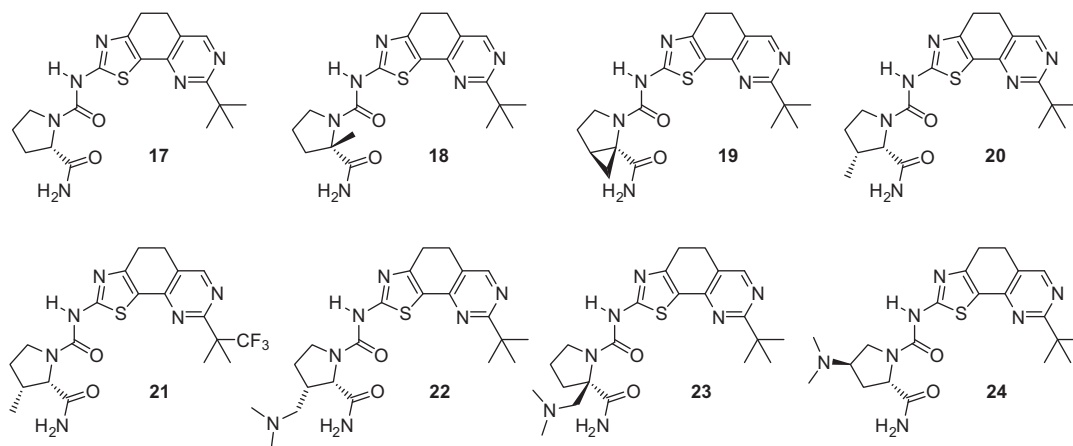
Scheme 1. Synthesis of the 4,5-dihydrobenzo[1,2-*d*:3,4-*d*]bisthiazole analogues **2**. Reagents and conditions: (i) thiourea, EtOH, 80 °C, 4 h (32–52%); (ii) Ac₂O, reflux, 2 h (81–84%); (iii) Br₂, AcOH, 75 °C, 18 h (82–86%); (iv) R²C(S)NH₂, 0.02 equiv. (NH₄)₃PMo₁₂O₄₀, EtOH, reflux, 2.5 h (11–72%); (v) concd HCl, EtOH, reflux, 4 h (90–98%); (vi) carbonyl diimidazole (CDI), DCM, 25 °C, 36 h (49–95%); (vii) (*S*)-proline-amide derivative, Et₃N, DMF, 25 °C, 18 h (46–86%).



Scheme 2. Synthesis of the 4,5-dihydrothiazolo[4,5-*h*]quinazoline analogues **14**. Reagents and conditions: (i) 3 equiv LiHMDS, –78 °C, then HCO₂Me –78 to 25 °C, 24 h (81–95%); (ii) R²C(NH)NH₂, pyridine, sealed-tube, 160 °C, 17 h (29–38%); (iii) concd HCl_(aq), EtOH, 85 °C, 2 h (90–95%); (iv) CDI, DCM, 25 °C, 2 h (35–92%); (v) (*S*)-proline-amide derivative, Et₃N, 2:1 CH₂Cl₂/DMF, 25 °C, 18 h (20–93%).

Table 4

PI3K α , PI3K β , PI3K γ and PI3K δ activities for the reference compound **13** and the 4,5-dihydrobenzo[1,2-*d*:3,4-*d*]bisthiazole analogues **17–24**



Compound	Biochemical IC ₅₀ (μM)				Cellular IC ₅₀ (μM)		
	PI3K α	PI3K β	PI3K γ	PI3K δ	PI3K α	PI3K β	PI3K δ
13	0.007	1.9	0.23	0.38	0.039	3.1	1.5
17	0.004	0.22	0.016	0.064	0.006	0.22	0.29
18	0.005	0.075	0.071	0.070	0.004	0.47	0.43
19	0.006	0.29	0.18	0.11	0.013	0.73	0.91
20	0.006	0.32	0.005	0.11	0.004	0.28	0.20
21	0.005	0.081	0.015	0.021	0.004	0.22	0.082
22	0.005	0.77	n.d.	n.d.	0.015	3.7	1.2
23	0.014	1.4	1.5	0.069	0.025	2.3	0.66
24	0.004	1.0	0.23	0.40	0.26	>10	4.4

observed for **7** versus **13**, when compared to the other class 1 PI3K isoforms, and this was also apparent for the majority of the sub-series of the general structure **14**. Small quaternary alkyl groups in the pyrimidyl 2-position, and the 2- and 3-methyl proline-amide variants were again found to provide the most potent PI3K α inhibitors, as exemplified by **18–21**. The *cis*-3-methylproline analogues, **20** and **21**, provided the highest level of potency for the sub-series **14**, as well as from our investigations into the whole 2-aminothiazole proline-amide-urea series. Incorporation of a tertiary amine, as a solubility enhancing moiety, was again explored at the proline 2-, 3- and 4-positions as exemplified by **22–24**.⁸ The 2- and *cis*-3-dimethylaminomethylproline analogues, **22** and **23**, in particular retained a high level of potency, with an acceptable level of selectivity versus the other class 1 PI3K isoforms.

Evaluating the physical properties of the 4,5-dihydrothiazolo[4,5-*h*]quinazoline analogues **14**, solubilities were again modest in the absence of the tertiary amino group (<125 μ M). More favorable was the combination of a moderately high permeability with high metabolic stability for these analogues, enabling good levels of rat oral exposure to be obtained, as exemplified by compounds **19** and **20** from Table 4. In particular, a low dose rat PK study with **19** resulted in an excellent oral bioavailability of 83% and particularly high exposure levels, as shown in Table 3. However, plasma protein binding measurements indicated lower free fractions in the rat for these analogues (<1%) compared to the other sub series: for example, free fractions of 0.4% and 6.0% were determined for compounds **19** and **13** respectively.¹⁷ As a consequence the increases in exposure, when expressed as free drug levels, were less dramatic, but were still significantly improved over the biaryl parent compounds. Interestingly, the serum albumin affinities indicated a higher level of binding in the rat compared to human and this was established to be the case (human PPB for **19**: 91.3%), but the extent of the high degree of binding in the rat was underpredicted by this method. The tertiary amine containing analogues **22–24** all showed higher solubilities. Compound **23** in particular proved interesting: the nitrogen atom in the β -position to the tertiary amine lowering the pKa to 6.6.¹⁸ The reduced basicity of compound **23** was considered a key factor in reducing the hERG activity, with no significant inhibition at concentrations up to 30 μ M, whilst the solubility at pH 6.8 remained high at >1 mM. High permeability and a reasonable level of *in vitro* metabolic stability were also measured for compound **23**, which resulted in good exposure and an oral bioavailability of 77% being obtained in a low dose rat PK study.

To further characterise the series **2** and **14**, the analogues were tested against an internal panel of 35 kinase assays, including the lipid kinases phosphatidylinositol-4-kinase beta (PI4K β), Vps34 and mTor. All the compounds exhibited no significant inhibition at concentrations up to 10 μ M in these biochemical assays, with the exception of PI4K β and Vps34, as exemplified for the analogues **5**, **10**, **12**, **18**, **20** and **23** in Table 5. These data support a high PI3K α selectivity for the series versus other kinases, with the PI4K β selectivity at a similar level to that within the class 1 PI3K family. Once

more an absence of mTor activity for the sub series **2** and **14** was determined, which was also evident in the parent biaryl series.

To increase the understanding of the interactions between the tricyclic series **2** and **14**, an X-ray structure was solved for compound **20** bound into the ATP-pocket of PI3K α , as shown in Figure 5.¹⁹ The structure revealed the expected binding interactions of the aminothiazole moiety within the hinge region, and for the proline-amide with the non-conserved PI3K α -specific Q859 residue.⁶ In addition, the starting hypothesis was validated with the methylene, introduced to close the central ring, making hydrophobic contacts with Y836.

To better understand the potential of the sub-series **2** and **14** as PI3K α inhibitors, pharmacodynamic (PD) studies were conducted in nude mice bearing Rat1-myr-p110 α xenografts.²⁰ The data from two separate studies with compounds **11** and **19** are shown in Figure 6. Similar mouse *in vitro* PK parameters were determined for both compounds: microsome extraction ratios of 69% and 47%; PPB levels of 89% and 90%, respectively, for **11** and **19**. In each study plasma levels and the extent of the inhibition of phosphorylation of Akt, on residue Ser⁴⁷³ (p-Akt) as a downstream readout of PI3K α inhibition, were measured at the indicated time points.

Compound **11**, dosed as a suspension, produced a PK profile which strongly suggested an extended absorption phase, consistent with the low solubility. Plasma concentrations above 1 μ M were measured up to 8 h post dosing for compound **11**, and were associated with a high level of inhibition of p-Akt. Compound **19**, dosed as a solution, produced a high plasma concentration at 8 h post dosing, which had fallen to 1 μ M after 16 h. The high level of variability seen in the plasma levels of **19**, at both time points, can also be assigned to the low solubility: potentially arising as a result of the compound precipitating in the gut, and leading to high variability in the extent of absorption. Inhibition of p-Akt for compound **19** was complete at 8 h after dosing and remained high after 16 h. For both compounds the correlation between free plasma concentration and the extent of p-Akt inhibition, in the context of the Rat1-myr-p110 α cellular IC₅₀ values, supported that the anticipated PK/PD relationship was operating.³ Furthermore, comparison of the levels of p-Akt inhibition obtained for **11** and **19**, with those observed for alpelisib, would predict both compounds to have the potential to inhibit the growth of PI3K α -dependent tumor-xenografts following chronic twice-daily dosing at, or close to, the above dose levels, assuming consistent exposure could be

Table 5
PI4K β and Vps34 activities for selected analogues from the series **2** and **14**

Compound	Biochemical IC ₅₀ (μ M)	
	PI4K β	Vps34
5	0.32	>9.1
10	0.21	9.6
12	3.2	>9.1
18	0.065	7.0
20	0.16	>9.1
23	4.0	>9.1

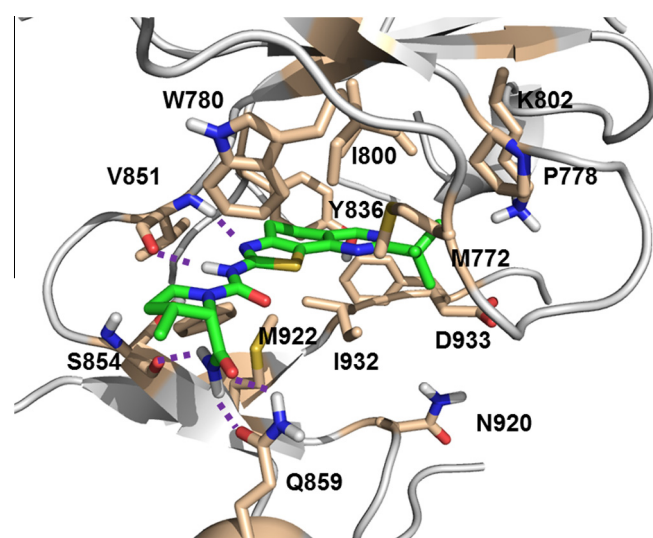


Figure 5. X-Ray structure of compound **20** bound into the ATP pocket of PI3K α , solved with a resolution of 2.8 Å. Only residues proximal to the inhibitor are represented. Key hydrogen bonds are represented as dashed lines.

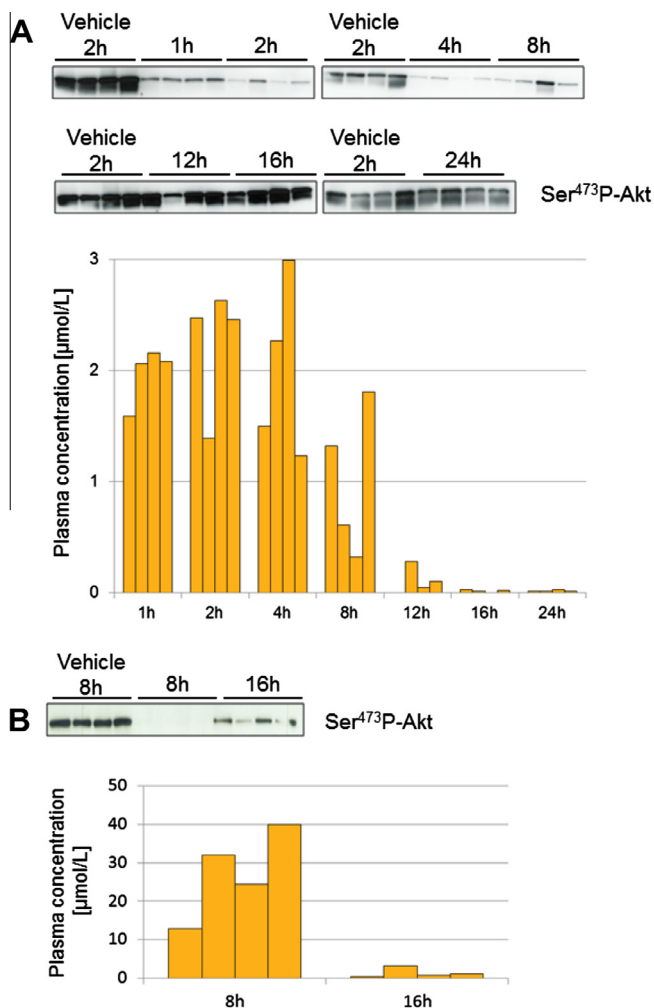


Figure 6. PK/PD relationships for compounds **11** and **19**. Female athymic mice bearing subcutaneous xenotransplants of Rat1-myr-p110 α tumors were treated with a single dose of 50 mg kg⁻¹, p.o of compound **11** (A) or **19** (B). At the indicated time points, the groups of mice ($n = 4$) were sacrificed, blood and tissues collected. Each tumor tissue was flash-frozen then pulverized and analyzed by Western blot to determine Ser⁴⁷³ p-Akt levels and in parallel the concentration of each compound was analyzed and quantified in plasma.

maintained.³ However, indications of solubility limited phenomena are apparent at the efficacious dose levels for both compounds in these and in other studies.

In conclusion, annulation of two biaryl series of (*S*)-proline-amide aminothiazole-urea PI3K α inhibitors generated the tricyclic series **2** and **14** which maintained the favorable selectivity profiles of the parent compounds, and additionally led to an increase in PI3K α potency. The rationale for this annulation was to strengthen the interaction with Y836, as a way to increase the affinity for the PI3K ATP-pocket, and the validity of this starting hypothesis has been supported by an X-ray structure of the cyclised analogue **20** within PI3K α . In addition, low dose rat PK studies have shown improved oral exposures for the annulated series, when compared to the biaryl parent compounds. PK/PD studies in the mouse with analogues from both of the sub-series **2** and **14** have shown them to be capable of inhibiting signaling through the PI3K pathway for greater than 8 hours, demonstrating their potential as in vivo PI3K α inhibitor tool compounds. However, a non-basic example which was not associated with some type of solubility-limited exposure was not identified from the sub-series **2** and **14**, and resulted in future efforts being focused upon retaining the

favourable potency and selectivity profiles of these tricyclic series whilst tackling the above limitation.²¹

Acknowledgements

The authors would like to thank Dorothea Haasen and Joerg Trappe for conducting biochemical assays, Peter Wipfli for performing bioanalysis and Werner Gertsch, Marijana Petrovic, Philippe Ramstein and Martin Kessler for their excellent technical assistance.

References and notes

- Polivka, J., Jr.; Janku, F. *Pharmacol. Ther.* **2014**, *142*, 164.
- Flanagan, J. U.; Shepherd, P. R. *Biochem. Soc. Trans.* **2014**, *42*, 120.
- Fritsch, C.; Huang, A.; Chatenay-Rivauday, C.; Schnell, C.; Reddy, A.; Liu, M.; Kauffmann, A.; Guthy, D.; Erdmann, D.; De Pover, A.; Furet, P.; Gao, H.; Ferretti, S.; Wang, Y.; Trappe, J.; Brachmann, S. M.; Maira, S.-M.; Wilson, C.; Boehm, M.; Garcia-Echheverria, C.; Chène, P.; Wiesmann, M.; Cozens, R.; Lehar, J.; Schlegel, R.; Caravatti, G.; Hofmann, F.; Sellers, W. R. *Mol. Cancer Ther.* **2014**, *13*, 1117.
- Fairhurst, R. A.; Imbach-Weese, P.; Gerspacher, M.; Caravatti, G.; Furet, P.; Zoller, T.; Fritsch, C.; Haasen, D.; Trappe, J.; Guthy, D. A.; Arz, D.; Wirth, J. *Bioorg. Med. Chem. Lett.* **2015**, *25*, 3569.
- Bruce, I.; Akhlaq, M.; Bloomfield, G. C.; Budd, E.; Cox, B.; Cuenoud, B.; Finan, P.; Geddeck, P.; Hatto, J.; Hayler, J. F.; Head, D.; Keller, T.; Kirman, L.; Leblanc, C.; Le Grand, D.; McCarthy, C.; O'Connor, D.; Owen, C.; Oza, M. S.; Pilgrim, G.; Press, N. E.; Sviridenko, L.; Whitehead, L. *Bioorg. Med. Chem. Lett.* **2012**, *22*, 5445.
- Furet, P.; Guagnano, V.; Fairhurst, R. A.; Imbach-Weese, P.; Bruce, I.; Knapp, M.; Fritsch, C.; Blasco, F.; Blanz, J.; Aicholz, R.; Hamon, J.; Fabbro, D.; Caravatti, G. *Bioorg. Med. Chem. Lett.* **2013**, *23*, 3741.
- (a) Brandl, T.; Maier, U.; Hoffmann, M.; Scheuerer, S.; Joergensen, A. T.; Pautsch, A.; Breitfelder, S.; Grauert, M.; Hoenke, C.; Erb, K.; Pieper, M.; Pragst, I. Preparation of dihydrothiazoloquinazolines as PI-3 kinase inhibitors. WO 2007/115929, Oct. 18, 2007.; (b) Betzemeier, B.; Brandl, T.; Breitfelder, S.; Brueckner, R.; Gerstberger, T.; Gmachel, M.; Grauert, M.; Hilberg, F.; Hoenke, C.; Hoffmann, M.; Impagnatiello, M.; Kessler, D.; Klein, C.; Krist, B.; Maier, U.; McConnell, D.; Reither, C.; Scheuerer, S.; Schoop, A.; Schweifer, N.; Simon, O.; Steegmaier, M.; Steurer, S.; Waizenegger, I.; Weyer-Czemilofsky, U.; Zoepfel, A. Preparation of thiazoloindazoles for treatment and prevention of cancer. WO 2006/040281, April 20, 2006.; (c) Breitfelder, S.; Maier, U.; Brandl, T.; Hoenke, C.; Grauert, M.; Pautsch, A.; Hoffmann, M.; Kalkbrenner, F.; Joergensen, A.; Schaenzle, G.; Peters, S.; Büttner, F.; Bauer, E. Preparation of fused thiazoles such as pyrazolobenzothiazoles, thiazolocyclopentapyrazoles, thiazolocycloheptapyrazoles, thiazoloquinazolines, and naphthothiazoles as PI3 kinase inhibitors. WO 2006/040279, April 20, 2006.
- Experimental details of the syntheses of the final products and intermediates are described. In: Fairhurst, R. A.; Gerspacher, M.; Mah, R. Preparation of carboxamidecycloaminoureathiazole derivatives for use as PI3-K inhibitors. WO 2011/000855, Jan. 6, 2011.
- Das, B.; Reddy, V. S.; Ramu, R. J. *Mol. Cat.* **2006**, *252*, 235.
- The biochemical (all four isoforms) and cellular (α , β and γ isoforms) PI3K activities were determined in the same manner as described in Ref. 4.
- Affinity for rat or human serum albumin, as a predictor of PPB, was measured using a chromatography method as described in: Reilly, J.; Etheridge, D.; Everatt, B.; Jiang, Z.; Aldcroft, C.; Wright, P.; Clemens, I.; Cox, B.; Press, N. J.; Watson, S.; Porter, D.; Springer, C.; Fairhurst, R. A. *J. Liq. Chromatogr. Relat. Technol.* **2011**, *34*, 317.
- Lorthois, E.; Marek, I.; Normant, J. F. *J. Org. Chem.* **1998**, *63*, 2442.
- Passive membrane permeability was assessed using a hexadecane membrane (HDM) permeability assay, as described in: Wohnsland, F.; Faller, B. *J. Med. Chem.* **2001**, *44*, 923; Data are expressed as the predicted fraction absorbed (FA) from the gastrointestinal tract following oral administration. The permeability of selected compounds was measured using Caco-2 monolayers, as described in: Pade, V.; Stavchansky, S. *J. Pharm. Sci.* **1998**, *87*, 1604.
- Solubility was measured using a high throughput equilibrium method at pH 6.8, as described in: Glomme, A.; März, J.; Dressman, J. B. *J. Pharm. Sci.* **2005**, *94*, 1.
- In vitro metabolic stability was measured, using the compound depletion approach, in rat liver microsomes from pooled rat hepatic microsomes preparations; microsomes (protein concentration 0.5 mg/mL) were incubated at 37 °C with the test compounds (1 μM) and the co-factor NADPH. Aliquots were removed at 0, 5, 15 and 30 min. Reactions were stopped by addition of acetonitrile and samples were subsequently analysed by LC-MS/MS after protein precipitation. The data were analysed as percentage disappearance of parent relative to the zero time sample, from which hepatic extraction ratios were determined.
- Rat pharmacokinetics: were conducted in female animals of the Sprague-Dawley strain; assessed blood levels from 5 minutes to 48 h post dosing; animals were conscious, permanently-cannulated with free access to food; doses of 1.0 and 3.0 mg kg⁻¹ were applied in the intravenous and oral arms respectively.

17. Plasma protein binding was measured by a rapid equilibrium dialysis method.
18. pKa values were determined by UV-absorbance changes as the test compounds are exposed to a calibrated pH gradient.
19. The single-crystal X-ray structure of compound **20** bound into PI3K α has been deposited with the Protein Data Bank ID: 4ZOP.
20. PK/PD studies were conducted with female athymic nude mice bearing Rat1-myr-p110 α xenografts, as described in: Maira, S.-M.; Pecchi, S.; Huang, A.; Burger, M.; Knapp, M.; Sterker, D.; Schnell, C.; Guthy, D.; Nagel, T.; Wiesmann, M.; Brachmann, S.; Fritsch, C.; Dorsch, M.; Chène, P.; Shoemaker, K.; De Pover, A.; Menezes, D.; Martiny-Baron, G.; Fabbro, D.; Wilson, C. J.; Schlegel, R.; Hofmann, F.; Garcia-Echeverría, C.; Sellers, W. R.; Voliva, C. F. *Mol. Cancer Ther.* **2012**, *11*, 317.
21. Gerspacher, M.; Fairhurst, R. A.; Mah, R.; Roehn-Carnemolla, E.; Furet, P.; Fritsch, C.; Guthy, D. A. *Bioorg. Med. Chem. Lett.* **2015**, *25*, 3582.